ICES Journal of Marine Science, 2024, Vol. 0, Issue 0, 1–11
https://doi.org/10.1093/icesjms/fsae156
Received: 10 May 2024; **revised:** 25 September 2024; **accepted:** 24 October 2024
Original Article

Forecasting and seasonal variability of the foot of the Shelfbreak Front in the Northern Middle Atlantic Bight

Adrienne Silver [1,*], Hilde Oliver [1], Glen Gawarkiewicz [1], Paula Fratantoni [2], Sarah L. Salois [3]

[1]Woods Hole Oceanographic Institution, 86 Water St, Woods Hole, MA 02543, United States
[2]NOAA Northeast Fisheries Science Center, 166 Water Street, Woods Hole, MA 02543, United States
[3]NOAA Northeast Fisheries Science Center, 28 Tarzwell Drive, Narragansett, RI 02882, United States

*Corresponding author. Physical Oceanography Department, Woods Hole Oceanographic Institution, 86 Water St, Woods Hole, Ma 02543, United States.
E-mail: adrienne.silver@whoi.edu

Abstract

The Shelfbreak Front in the Northern Middle Atlantic Bight delineates the boundary between colder, fresher shelf water and warmer, saltier slope water. The location of the foot of the Shelfbreak Front, where the frontal isohalines and isopycnals intersect the bottom, is highly dynamic, impacting several commercial fisheries. In this work, we present new indices to quantify seasonal and interannual variability in the movement of the foot of the Shelfbreak Front. One index is generated from over three decades of observational Conductivity, Temperature, and Depth (CTD) data, and the other from GLORYS reanalysis fields. After detrending and removing seasonality, both indices capture similar variability and were found to be statistically significantly correlated with upstream along-shelf geostrophic velocities derived using satellite altimetry data. Using the lag correlation between the along-shelf geostrophic velocities from the Scotian Shelf to Georges Bank, skillful forecasts for the frontal indices were obtained up to three seasons in advance. This work provides a useful methodology for including variability of the foot of the Northern Middle Atlantic Bight Shelfbreak Front into ecosystem and stock assessment models using readily available near-real-time satellite altimetry data.

Keywords: Shelfbreak Front; forecasting; seasonal variability; ecosystem management

Introduction

The Northern Middle Atlantic Bight Shelfbreak Front is a water mass boundary separating the cool fresh waters of the continental shelf from the warm saline waters of the continental slope (Linder and Gawarkiewicz 1998). This front marks an important faunal boundary due to the large temperature contrast across the front (4–6°C) and theorized persistent upwelling along frontal isopycnals (e.g. Gawarkiewicz and Chapman 1992, Houghton and Visbeck 1998, Zhang et al. 2013). In addition to the watermass separation, the sharp density gradient generates a surface intensified along-shelf jet, which is a part of the large-scale current system extending from the Labrador Sea to Cape Hatteras (Fratantoni and Pickart 2007)).

The Shelfbreak Front in this region is important to numerous commercial fisheries, with the shelf waters in the region supporting two of the nation's top fishing ports by volume and value (New Bedford, MA, USA and Reedville, VA, USA; National Marine Fisheries Service 2024). The front's impact on fishing can be seen by the fishing vessel activity in the region, showing significant occupation of the Shelfbreak Front (e.g. from the Global Fisheries Watch website). In addition to the Shelfbreak Front acting as a biological hot spot, shoreward movements of the front can cause rapid temperature shifts that significantly impact benthic species such as lobster, flounder, and scallops (Miller et al. 2016b, Tanaka et al. 2020). The Shelfbreak Front's cross-shelf movements are extreme and may result in onshore/offshore movements of up to 30 km in 2 days (Houghton et al. 1994).

Understanding the variability and forecasting the position of the Shelfbreak Front is becoming increasingly important in predicting and managing related ecosystem services within the shelf waters. In recent years, the New England shelf waters have experienced accelerated warming (Forsyth et al. 2015, Pershing et al. 2015, Kavanaugh et al. 2017). Harden et al. (2020) found that the shelf waters south of Cape Cod warmed by 0.26°C/year from 2003 to 2013 in early summer, leading to a significant increase in stratification. At the same time, an increase in the number of warm core rings forming off the Gulf Stream led to an increase in intrusions of warm salty slope water across the shelfbreak (Gangopadhay et al. 2020, Gawarkiewicz et al. 2022, Silver et al. 2023). The effect of the changing water properties over the shelf and increased offshore forcing from the Gulf Stream on the position of the Shelfbreak Front has yet to be examined over longer time and shelf-wide spatial scales. As the slope water temperatures increase due to greater influence from the Gulf Stream (Silver et al. 2021), these cross-shelf movements could drive marine heat waves (e.g. Gawarkiewicz et al. 2019), having large impacts on the shelf ecosystem (Mills et al. 2013, Smith et al. 2021).

The real-time position of both the surface and bottom expression (also called the foot) of the Shelfbreak Front is difficult to quantify. The surface expression of the front is difficult to locate in the summer due to the generation of the seasonal thermocline, which can wash out the cross-shelf gradients at the surface. Using an edge detection algorithm to identify oceanographic fronts in the Northwest Atlantic, Ull-

man and Cornilion (1999) found that the surface signature of the Shelfbreak Front south of Hudson Canyon completely disappeared in the summer. Additionally, the relationship and variability between the surface signature and the foot of the front is poorly understood. Wright (1976) noted that the surface expression of the front was much more variable than the expression at depth, which typically stayed within 10 km of the 100 m isobath. In a more recent study, Chen et al. (2022) documented a bottom intrusion extending 100 km shoreward of the shelfbreak (roughly the 100 m isobath), with the surface signature remaining offshore. These changing dynamics make the foot of the front particularly difficult to quantify without *in situ* measurements at depth.

The frontal structure is also related to the movements of the Shelfbreak Jet, which is unstable and prone to rapid movements. The position of the front, as measured by either its surface or bottom expression (also called the foot), may be tied to the current signature in the Shelfbreak Jet. Numerous previous studies have assessed subsurface variability in the position of the Shelfbreak Front and jet at specific locations along the shelfbreak using either shipboard measurements or mooring data (Pickart et al. 1999, Fratantoni and Pickart 2003, Gawarkiewicz et al. 2004, Flagg et al. 2006, Forsyth et al. 2020). Though these studies resolve frontal movement, they are limited in both temporal and spatial extent.

Here, we examine the seasonal and interannual movement of the bottom signature of the water mass boundary between the shelf and slope waters, an approximation of the foot of the Shelfbreak Front, over 32 years across the Middle Atlantic Bight. We focus on the foot of the front due to its importance to the habitat of benthic species and due to the lack of understanding of its movement over decadal timescales. This was done using observational CTD data collected across the Middle Atlantic Bight shelf and model reanalysis output from the GLORYS reanalysis product to generate two different indices quantifying the position of the foot of the Shelfbreak Front.

We then apply a physics-based approach to forecast the position of the foot of the Shelfbreak Front. Wright (1989) considered a two-layer surface-to-bottom density front, with the front separating fresher coastal water from denser offshore water. He found that the position of the front moves offshore until it reaches the shelfbreak, where the bottom boundary layer transport is reduced, and the offshore movement of coastal fresh water is halted. Building on this work, Chapman and Lentz (1994) used a similar model but allowed for density advection in which the along-shelf velocities can affect the bottom boundary layer. The conceptual model presented by Chapman and Lentz (1994) is as follows. As the inflow moves along the shelf, a bottom Ekman layer is formed with less dense, fresher water flowing offshore along the bottom and a compensating onshore flow above made of denser, saltier water. This instability then undergoes convective adjustment, leading to a sharp density front. The front also geostrophically adjusts, generating a surface intensified along shelf jet. This process continues to move the front further offshore with the front and jet maintaining their spatial structure. Due to the vertical velocity shear remaining constant within the jet, the along-shelf velocity at the bottom decreases as the front moves offshore. Eventually, a depth is reached in which the bottom along shelf velocity reaches zero, or even becomes negative. This change in the bottom along shelf velocities impacts the bottom boundary layer so that the bottom offshore flow only occurs inshore of the density front (where bottom along shelf velocity is still positive), halting the offshore buoyancy flux and preventing the front from moving further offshore. Yankovsky and Chapman (1997) used this conceptual model by Chapman and Lentz (1994) to generate a simple theory explaining the vertical structure and offshore spread of buoyant inflow onto a continental shelf. In their theory, as in Chapman and Lentz (1994), the offshore movement of the front is driven by the frictional bottom boundary layer, with the front becoming trapped when the bottom along-shelf velocity equals zero. Yankovsky and Chapman (1997) call this depth the equilibrium depth (h_b), which can be thought of in this work as the depth of the foot of the front. Yankovsky and Chapman (1997) then derive an equation for h_b using the inflow transport and the Coriolis parameter with $h_b = \sqrt{2Lvh_0 f/g'}$. Here L, h_0, and v are the width, depth, and uniform velocity of the buoyant flow, respectively, f is the Coriolis parameter, and g' is reduced gravity.

We explore this theory presented by Yankovsky and Chapman, utilizing the generated front indices as an approximation of the equilibrium depth (h_b) and surface geostrophic velocity from satellite sea surface height gradients as an approximation of v. From this relationship, we develop a forecasting model and discuss possible future applications of such indices for fisheries and ecosystem management.

Data

The position of the foot of the Shelfbreak Front was investigated using both multi-decadal observational data and a model reanalysis product. CTD data was taken from the World Ocean Database (WOD) from 1990 to 2021 in the region bounded by 75–65°W and 35–43°N (Boyer et al. 2018). Most of these profiles were collected by the Ecosystem Monitoring Program (EcoMon), which is run by the National Oceanic and Atmospheric Administration's Northeast Fisheries Science Center. EcoMon cruises take place up to six times per year, with each cruise collecting CTD profiles at 120 randomly selected stations and 35 repeat stations across the shelf and slope from Cape Hatteras, NC, to Cape Sable, Nova Scotia. In total, there were 62 383 available CTD profiles within the study region collected between 1990 and 2021. Supplementary Fig. S1 shows the spatial distribution of these profiles per season. The reanalysis product used was the GLORYS12V1 product (GLORYS) taken from Copernicus Marine Services (doi: https://doi.org/10.48670/moi-00021), with gridded fields spanning 1993–2020. GLORYS is a global ocean eddy-resolving reanalysis with 1/12° horizontal resolution. This product uses the NEMO platform as the model component and is forced at the surface by either ECMWF ERA-Interim wind stress and heat flux for early years or ERA5 for more recent years. GLORYS assimilates *in situ* temperature and salinity, sea surface temperature, along-track altimeter, and sea ice concentration data using a reduced-order Kalman filter. Castillo-Trujillo et al. (2023) found that the GLORYS reanalysis was one of the most accurate reanalysis products for bottom temperature and salinity within the New England shelfbreak region. The GLORYS reanalysis was also recently used to create statistical predictions of the Northeast US shelf bottom temperatures (Chen et al. 2021). Gridded daily sea surface height extracted from Copernicus Marine Services was used to derive along-shelf velocities from 1993 through 2021 (https://doi.org/10.48670/moi-00148).

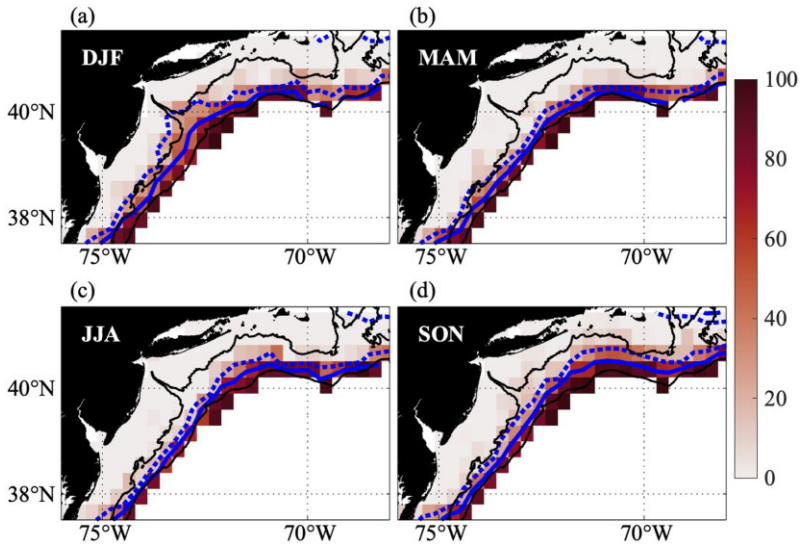

Figure 1. Bottom slope water frequency maps, with shading showing the percentage of CTD profiles within the region that contain the bottom signatures of slope and front water for the four seasons Winter, Spring, Summer, and Fall shown in subplots (a), (b), (c), and (d), respectively. The thick solid and dashed blue lines show the 50% and 20% contour lines, respectively. The thin black lines show the 100 m and 50 m isobaths.

Developing metrics for variability in the position of the foot of the Shelfbreak Front

Seasonal variability in the cross-shelf position of the foot of the Shelfbreak Front

Using the CTD data, frontal variability was investigated by generating "bottom slope water frequency maps" with a 0.3 by 0.3-degree resolution. Slope water frequency was calculated as the number of profiles per bin containing the bottom salinity threshold (salinity >34) out of the total number of profiles in each bin (Supplementary Fig. S1 shows the total number of profiles per bin). Frequencies were then multiplied by 100 to be represented as a percentage. The threshold of bottom salinity >34 was used as it marks the water mass boundary between the typical shelf water (salinity <34, Manning 1991, Mountain 2003) and the offshore Slope Sea waters. This isohaline is also typically associated with the inshore edge of the density-driven Shelfbreak Front. Only the salinity at the bottom of each profile was considered to understand the movement of the foot of the front. It should be noted that shipboard CTD profiles are not able to capture the true bottom salinity at the sea floor due to concern for the instrument being damaged. Comparing the bottom salinity measurements to the ETOPO Global Relief Model bathymetry data (Amante and Eakins 2009), it was found that the difference between the bathymetric depth and the bottom salinity measurement has a mean of 6.3 m and a median of 4 m (see Supplementary Fig. S2). The distance the bottom CTD measurement was above the sea floor was also typically greater in deeper waters off the shelf break, particularly around the 500 m depth.

Frequency maps were generated for the four different seasons grouped as December through February, March through May, June through August, and September through November (Fig. 1). The mean position of the foot of the front can then be inferred from the high gradient in frequency as you move inshore, indicating the boundary between the regions with bottom signatures typically containing front/slope versus shelf waters. This high gradient is found near the 100 m isobath for all four seasons, matching previous observations of the position of the foot of the Shelfbreak Front (Linder and Gawarkiewicz 1998, Gawarkiewicz et al. 2018). The 20% and 50% contour lines shown in blue in Fig. 1 help highlight seasonal variability within the front position. In winter, higher frequencies of front/slope waters are observed up to the 50 m isobath centered around the Hudson Canyon and Hudson Shelf Valley. By contrast, in the fall front/slope water is observed moving inshore south of Nantucket Shoals.

Generation of a foot of the front index

The Shelfbreak Front is created by the sharp temperature and salinity gradients where the shelf and slope waters meet. The front contains cross-shelf density gradients giving rise to an alongshelf geostrophic jet, typically called the Shelfbreak Jet (Fratantoni et al. 2003). Given the limitations of observational data, generating a 2D map of across shelf gradients along a stretch of longitudes is not realistic. To work around this, a specific isotherm, isohaline, or isopycnal is often selected as a marker of front position (Wright 1976, Fladd and Beardsley 1978; Linder and Gawarkiewicz; Joyce et al. 1992, Zhang et al. 2023). We decided to use the 34 isohaline, which marks the edge of the shelf water mass and is typically associated with the inside edge of the Shelfbreak Front. To test the sensitivity of the isohaline selection, we regenerated the indices using the 34.5 isohaline, yielding similar results with r^2 values of 0.84 and 0.97 between indices generated from CTD and the GLORYS reanalysis, respectively (see Supplementary Fig. S3).

The WOD CTD profiles were used to create an observational foot of the front index (FFI), tracking the relative seasonal position of the water mass boundary between shelf and slope waters typically associated with the foot of the Shelfbreak Front. This index was constructed for each season between 1990 and 2021. To create the FFI, CTD profiles were first sorted, identifying the subset that reported bottom salinity ≥34 indicative of slope or frontal water. From this, the maximum onshore extent of the front was calculated for each season by identifying the northernmost profile within each

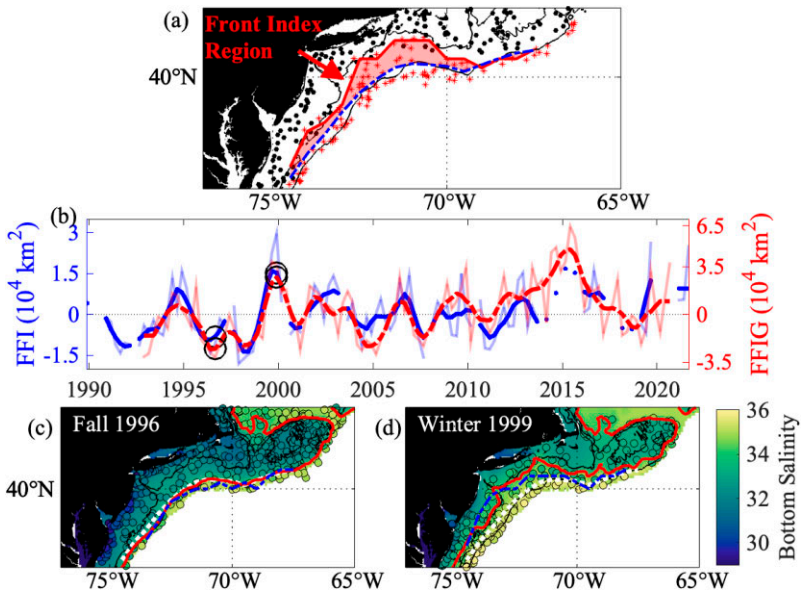

Figure 2. (a) Schematic showing the calculation of the FFI. Dots show locations of CTD profiles with red asterisks containing the signature of the front. The thick red line shows the maximum extent position of the front, and the dashed blue line shows the mean position. The shaded red region then shows the integral area from which the front index is calculated. (b) The time series of FFI (blue) and FFIG (dashed red) with the bold lines showing the de-seasoned time series (the long-term trend has not been removed) and the faded lines showing the raw indices. Note the different y-axis for the two time series, accounting for the difference in range. Black circles mark the years that are shown in (c) and (d). Subplots (c) and (d) show the positions of the foot of the Shelfbreak Front for Fall 1996 and Winter 1999, respectively. Shading shows bottom salinity with the background shading from GLORYS and the dots showing CTD profiles from the WOD. The solid red line marks the position of the 34 isohaline from GLORYS data, and the dashed blue line shows the maximum extent location of the front from WOD CTD data. The white dotted line shows the mean position of the front from all 32 years of WOD CTD data. The thin black contour lines show the 100 m and 50 m isobath.

0.1-degree bin along the shelfbreak that contained slope water (see Fig. 2a). The seasonal average position of the front was then computed as the seasonal average position of all maximal locations. The FFI was derived by calculating the area between the maximum extent of the front for a given season to overall mean position of the front. Areas where the maximum extent was south of the mean had negative integrals, and areas where the maximum extent was north of the mean had positive integrals. This index has units of km^2 representing the cumulative area above or below the mean (having positive and negative values, respectively). Given the patchiness of the CTD data in space and time, seasons in specific years were excluded from the index if there were no CTD profiles containing the signature of the front for more than half of the longitudinal bins.

Given the patchy nature of the observational index caused by gaps in the available CTD data, an alternative foot of the front index (FFIG) was generated from seasonally averaged GLORYS reanalysis fields from 1993 to 2020. In the gridded GLORYS fields, the position of the foot of the front was identified as the 34 isohaline in bottom salinity. The mean position of the front was then calculated as the average position of all 34 isohalines in a given season through the 31-year time series. As with the FFI, the alternative index (FFIG) was generated as the area between the position of the front in a given season and the overall mean position, having units of km^2. Though the FFI and FFIG are generated using similar methodologies, it is important to keep in mind the different biases inherent in the two different datasets. The WOD CTD data is nonuniform in space and time. Each CTD profile reports an instantaneous snapshot of the bottom salinity at a specific location and time. From this, the shoreward-most position of the front is found from multiple individual snapshots. These instantaneous measurements are influenced by the short-term variability in the front's position, potentially aliasing the front's true variability. To help decrease this bias, only seasonal indices were calculated to increase the sample size of profiles on the shelf. The FFIG, on the other hand, is generated from the seasonal mean position of the front taken from gridded reanalysis fields that do not have the same patchiness as the CTD data. These reanalysis fields have their own biases that are described nicely in Castillo-Trujillo et al. (2023). The bias in bottom salinity in the region seems to be relatively small and uniformly negative (see Castillo-Trujillo et al. 2023). This suggests that the error in estimating the relative movement of the front should be minimally affected by the model biases .

Comparison of front indices and interannual variability

To compare both indices, the seasonality was first removed. The seasonality was removed with a centered five-season moving average, with the endpoints having half the weight. For example, the de-seasoned index value for time t and season x would have the value $\frac{1}{8}x_{t-2} + \frac{1}{4}x_{t-1} + \frac{1}{4}x_t + \frac{1}{4}x_{t+1} + \frac{1}{8}x_{t+2}$. For the FFI, data gaps were filled using linear interpolation before the moving average was applied. The missing seasons were then removed from the de-seasoned time series.

After the seasonality is removed, the FFIG shows similar variability to the FFI, with both indices showing covarying peaks and troughs with a correlation coefficient of $r = 0.75$ with $P < 0.0001$ once both indices are detrended (Fig. 2b). Breaking the time series into individual seasons also revealed strong correlations, with r values of 0.74, 0.77, 0.74, and 0.74 for winter, spring, summer, and fall, respectively.

The estimated area above or below the mean position of the front is almost double in the FFIG than that estimated

from observations. The FFIG shows a much larger fluctuation in magnitude, with a minimum value of $-26\,000\,km^2$ in the summer of 1996 and a maximum in the summer of 2015 of $48\,000\,km^2$. Meanwhile, the FFI shows a minimum value of $-14\,000\,km^2$ in the summer of 1998 and a maximum of $17\,000\,km^2$ in the spring of 2015. Both indices show a statistically significant increasing trend with slopes of 230 and $80\,km^2$ season^{-1} for the FFIG and FFI, respectively. Given the mean length of the front in the index region (~730 km), the increasing trend in the two indices equates to a total inshore movement of the front of ~35 km estimated from the FFIG and ~14 km estimated from the FFI across the whole index region. When both indices are normalized to account for the larger range in the FFIG, the trends are roughly the same (0.015 and 0.011 season^{-1} for the FFIG and FFI, respectively).

The FFI and FFIG indices show substantial interannual variability. For example, in the fall of 1996, both indices have low values, indicating that the front is located further offshore (Fig. 2c). This can be seen in the bottom salinity of GLORYS and the CTD profiles, with values of 34 being found around or offshore of the 100 m isobath (see Fig. 2c). In contrast, in the winter of 1999, the CTDs show a large inshore movement of the front (Fig. 2d). During this time the bottom salinity in the GLORYS and CTD data show the signature of the front inshore of the 50 m isobath (Fig. 2d).

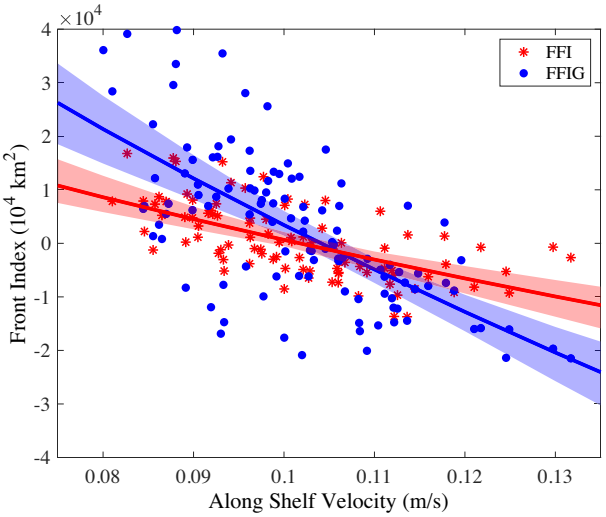

Figure 3. The along-shelf geostrophic velocity in Region 1 compared to the two front indices, blue dots being the FFIG and red asterisk being the FFI. The blue and red lines show the square root models generated from the 100-resample bootstraps for the FFIG and FFI, respectively. The shaded region around each line shows a range in the model derived from the 100-resample bootstrap.

Forecasting model for the foot of the Shelfbreak Front

Along shelf transport as a forcing mechanism for frontal movement

We apply a physics-based approach to forecast the location of the foot of the Shelfbreak Front. Yankovsky and Chapman (1997) derive an equation for h_b (the equilibrium depth) using the inflow transport and the Coriolis parameter with $h_b = \sqrt{2Lvh_0 f/g'}$. Here L, h_0, and v are the width, depth, and uniform velocity of the buoyant flow, respectively, f is the Coriolis parameter, and g' is reduced gravity. This theory ignores the ambient shelf circulation, tides, and wind forcing.

Based on this theory, we hypothesize that the position of the Shelfbreak Front relates to the along-shelf surface velocity in the region adjacent to our study area. Based on the conceptual model from Chapman and Lentz (1994; discussed in "Introduction") and the equation presented by Yankovsky and Chapman (1997), assuming the vertical velocity shear in the shelf break jet remains constant, theory predicts that a stronger along shelf velocity at the surface will lead the bottom along shelf velocity to decrease to zero deeper in the water column, and therefore the equilibrium depth would also be deeper. Assuming L, h_0, f, and g' are roughly constant, we simplify the above equation to $h_b \approx C\sqrt{v}$, where C is a constant. To investigate this relationship, we used geostrophic surface velocities derived from sea surface height as an approximation for v and compared these to our front indices generated in the section "Developing metrics for variability in the position of the foot of the Shelfbreak Front," which we used as an approximation for h_b.

The geostrophic surface velocities were isolated in a region adjacent to our index region using the 500 m isobath as the offshore edge, extending 0.75° inshore and spanning 2.5° longitude (see Fig. 4a, Region 1). This region can be thought of as our "inflow" region, in which v will be derived. For each season in the 31-year time series, the surface velocities in this region were isolated, and the along-shelf flow was derived using the 500 m isobath as the along-shelf direction. Note that mean along shelf flow always travels in the southwest direction. Throughout the paper, we will use positive values to represent this flow, with higher values meaning a stronger flow in this southwest direction.

To accurately compare the relationship between the two front indices and the along-shelf geostrophic velocities (ASGV), all variables were detrended, and the seasonality was removed using a centered five-season running average explained above. From these detrended variables, models of the form $h_b = m\sqrt{v} + b$ were fitted using a 100-resample bootstrap. The bootstrap analysis was done by generating 100 new v and h_b variables by randomly selecting seasons from the original v and h_b with replacement, generating 100 new variables of the same length. From each of these 100 resamples the model coefficients and model fit statistics such as r^2 and root mean squared error (RMSE) were calculated. Coefficients and model fit statistics shown throughout the paper represent the mean of these 100 resamples.

Figure 3 shows the results of these square root models for both indices. The r^2 values for the FFI and FFIG models are 0.40 and 0.44, respectively. Though the ASGV explains roughly the same amount of variance in the FFIG and the FFI, both models have distinctly different coefficients, partly generated by the much larger range in the FFIG.

Generating a forecasting model

The ASGV at the Tail of the Grand Banks of Newfoundland have been found to have a lagged correlation with the ASGV as far south as the Great South Channel, the location of our "in flow region," Region 1 (Neto et al. 2021). Using this lagged relationship between the ASGV at Great South Channel and the ASGV at the Scotian shelf, and applying the model introduced above, it may be possible to forecast the frontal position several seasons in advance. To generate this forecasting model,

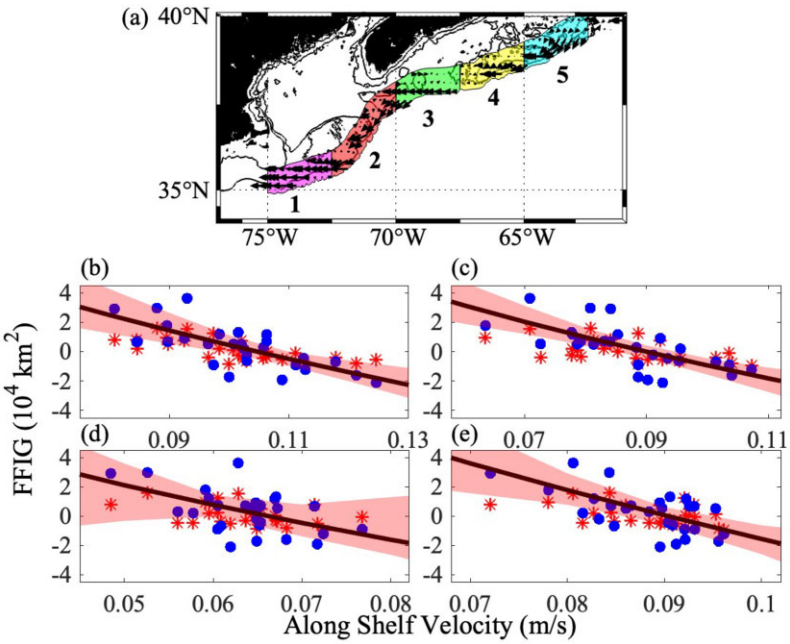

Figure 4. (a) Map showing the five regions in which the ASGV were calculated. Vectors show the along-shelf component of the geostrophic velocities. Black contours show the 100 and 50 m isobaths. (b) Relationship between the foot of the Shelfbreak Front Indices (blue dots being the FFIG and red asterisks being the FFI) in fall and the ASGV. Model trends are derived from 100-sample bootstrap of the FFIG and the ASGV. The red-shaded region shows the range in the models from these bootstraps. (c–e) Same as (b) but with one- and three-season lags, respectively.

we created four new ASGV regions extending to the northeast of Region 1 along the 500 m isobath, each spanning 2.5° longitude (see Fig. 4a Regions 2–5). We find that the lag time with the highest correlation between Regions 5 and 1 is 9 months, matching what was found in Neto et al. (2021) (see their Fig. 3) and allowing for forecasts three seasons in advance.

Because of the patchiness of the FFI time series, we will present forecasting models generated using FFIG; however, all analyses were repeated with the FFI yielding similar results with, on average, slightly lower r^2 values (Supplementary Fig. S4). Each season was examined separately to remove the autocorrelation in both time series and to better understand how seasonal differences affect the lag relationship between the FFIG and ASGV. For each season, a different model was created for each of the five ASGV regions with up to a three-season lag. For example, 20 models were created for the FFIG in winter, with one model for each region, with each seasonal lag period (zero-, one-, two-, and three-season lags). This process was then repeated for spring, summer, and fall. Results from these models for fall are shown in Fig. 4b–e for lags of zero through three seasons. Figure 5 then shows the r^2 and RMSE results for all models.

A significant model fit is found for all seasons with the ASGV in Regions 1 and Region 2 with no lag (Fig. 5a–d), matching what would be expected from the mechanisms proposed in Yankovsky and Chapman (1997), and what is found in Fig. 3. Region 2 shows the strongest correlation with no lag with mean r^2 values of 0.51, 0.47, 0.54, and 0.57 for winter, spring, summer, and fall, respectively. For a one-season lag, the strongest correlation with all seasons was between the FFIG and the ASGV in Region 2 (r^2 of 0.50, 0.45, 0.45, and 0.46 for winter, spring, summer, and fall, respectively). For periods of higher lags of two to three seasons, the region of ASGV showing the strongest correlation with the FFIG varies, ranging from Region 2 to Region 5. For all seasons, the correlation between the FFIG and ASGV weakens with two- and three-season lags. This can be seen by the error bars on the r^2 values overlapping with the significant line in the two- and three-season lag boxes (Fig. 5i–p). Except for summer (Fig. 5k and o), all seasons of FFIG show a significant mean r^2 value with at least one region of ASGV for both two- and three-season lags.

Discussion

We have generated observational and reanalysis indices that capture the variability in the position of the foot of the New England Shelfbreak Front. Both indices show substantial interannual variability, highlighting seasons when the shelf water might have been largely influenced by the inshore movement of the front. In addition, both indices have significant increasing trends of similar scale once normalized. Given that both indices are generated using a constant isohaline as a marker of the front position, it is possible that this increasing trend could be due to the salinification of the shelf and slope waters. More work will need to be done to see if this inshore movement is observed in measures of the shelfbreak density front and the shelfbreak jet. From these indices, we were then able to create forecasting models that can forecast the position of the foot of the front up to three seasons in advance using the geostrophic velocities derived from satellite sea surface height data. The simplicity of these models and the fact that they use near-real-time satellite data make them a potential metric to be included within future ecosystem and stock assessments. It should also be noted that linear models can be used instead of the square root model (from the Yankovsky–Chapman theory) for simplicity in practical applications, yielding similar results.

Other potential drivers of frontal variability

The models generated using the hypothesis presented in Yankovsky and Chapman (1997) explain roughly 40%–50%

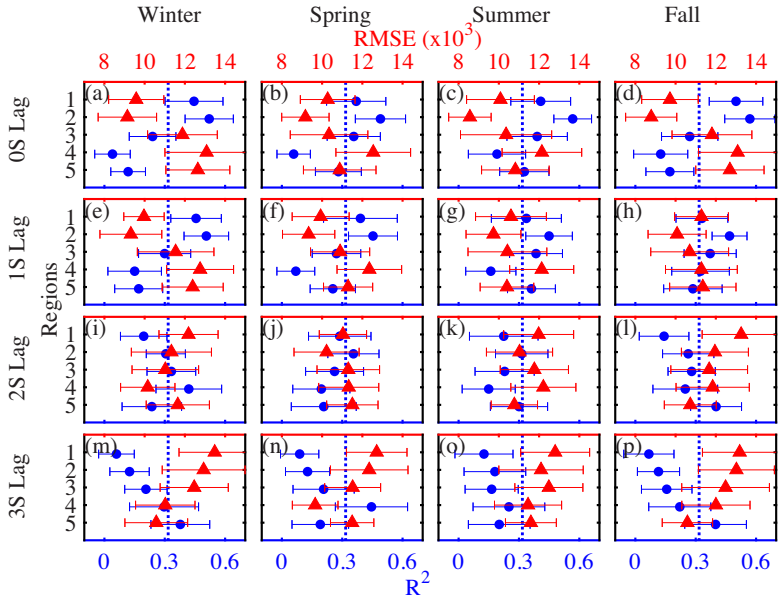

Figure 5. The average r^2 (blue dot) and RMSE (red triangle) values each group of 100 bootstrap resamples comparing the FFIG to the square root model output. Error bars represent the standard deviation from the 100 bootstrap resamples. The four columns show the four different seasons (winter, spring, summer, and fall), and the four rows show different lag periods, zero-, one-, two-, and three-season lags. In each subplot, the five rows represent the different regions of the ASGV being compared to the FFIG. The vertical blue dotted line represents the significance boundary for the r^2 values, with r^2 higher than the dotted line being significant at the 95% confidence level.

of the variance in the front indices. Though these results show substantial value in explaining the variability in frontal movement through a simple model (discussed further in the section "Applications for fisheries and ecosystem management"), a large portion of the front variability remains unaccounted for. One large assumption made in Yankovsky and Chapman (1997) is that wind forcing is ignored. Houghton et al. (1988) noted that wind-driven Ekman forcing could shift the front inshore during the winter by around 10–20 km on periods ranging from 2 to 25 days. This length scale of 10–20 km matches the inshore movement we see in the winter from the slope water frequency maps (Fig. 1a). Beardsley et al. (1985) found a similar relationship between local winds and frontal fluctuations. In an extreme example, Chen et al. (2022) found that upwelling favorable winds and cyclonic ringlets along the shelfbreak helped force a bottom-intensified intrusion across the Shelfbreak Front leading to an advective marine heatwave. Future work needs to be done to see how wind forcing could affect the position of the front on the longer seasonal time scales examined in the two front indices.

Another potential driver of frontal variability not included in the Yankovsky and Chapman (1997) model is offshore forcing from the Gulf Stream system, particularly by warm core rings. Past studies have found mixed relationships between warm core rings and the position of the Shelfbreak Front. For example, Fratantoni and Pickart (2003) and Beardsley et al. (1985) both used mooring data to look at frontal variability around Nantucket Shoals. However, Fratantoni and Pickart (2003) found no significant impact of rings on the cross-shelf position, whereas Beardsley et al. (1985) found that warm core rings could push the front shoreward. The discrepancies between these two papers could be partly due to the short time scales of both studies and the large variability in warm core ring properties. Forsyth et al. (2020 and 2022) examined the relationship between warm core rings and the Shelfbreak Jet position using ADCP data from the MV Oleander. They found that warm core rings could shift the front inshore and that rings that had faster rotational velocities and that were closer to the shelfbreak had a larger influence. Given the large range in size (radius ranging from 50 to 150 km) and lifespans (2–25 weeks or longer) of warm core rings (Gangopadhyay et al. 2020), it will be important moving forward to examine both the presence of rings as well as the ring properties when investigating their influence on the Shelfbreak Front. Additionally, Silver et al. (2022) showed that there are different types of warm core rings that form off the Gulf Stream through different formation processes (classic pinch-off versus aneurysm) that could have varying impacts on the Shelfbreak Front. Understanding the relationship between the front position and warm core rings could be important in explaining the increasing trend found in both indices. Gangopadhyay et al. (2019) found that the number of warm core rings forming off the Gulf Stream has undergone a regime shift, doubling after the year 2000. This increased influence of warm core rings along the shelfbreak could cause the front to move further inshore in recent years and remain inshore for extended periods of time. In particular, there was high ring occupancy along the shelfbreak in the Middle Atlantic Bight region around 2014 and 2015 (Silver et al. 2023, see Supplementary Fig. S1), potentially contributing to the high FFIG during this period. In addition, the higher formation rates of warm core rings in summer (Gangopadhyay et al. 2019, Silver et al. 2021) might contribute to the weaker forecasting ability during

these months and the front moving further inshore in the fall (Fig. 1d).

Applications for fisheries and ecosystem management

The significant relationship between the position of the foot of the Shelfbreak Front and the along-shelf velocities has substantial practical applications that could play an important role in future ecosystem and stock assessments. The position of the Shelfbreak Front is hard to measure at the surface in the summer and fall due to atmospheric warming and seasonal stratification washing out the temperature gradient signal. Additionally, the relationship between the surface and the foot of the front is not well understood. This work provides an alternative methodology for including frontal variability in ecosystem and stock assessment models using readily available near-real-time satellite data. Such an understanding of frontal variability could be crucial to understanding the population dynamics of commercially important benthic species.

Temperature will play a significant role in future species distribution and abundance (Kleisner et al. 2017, Morley et al. 2018). The thermal gradient across the Shelfbreak Front can generate rapid changes in bottom temperature as the front moves inshore. As the oceans warm and the Slope Sea temperatures increase, these sharp temperature changes associated with the front could push species outside their range of habitable temperatures. For example, scallops, one of the most economically important fisheries in the New England shelf region, have optimal growth rates at temperatures between 10 and 15°C, with mortality greatly increased around 21°C (Stewart and Arnold 1994). The typical temperature increase across the front of 4–6°C could push these species out of their optimal growth range. Changes in the Shelfbreak Front position can also lead to shifts in predator-prey dynamics. For example, the front acts as a thermal barrier for the sea star *Astropecten Americanus*, a predator of scallops (Hart 2006). Inshore movement of the front further into scallop habitat could, therefore, lead to higher predation rates. Further, beyond temperature, a shift in the Shelfbreak Front delivers dramatically different water mass properties, which can lead to osmoregulatory stress and changes in stratification, food, and nutrient availability (McHenry et al. 2019). For some species, inshore movement of the front can be advantageous. For example, Black Sea Bass overwinter in the warmer, saltier waters of the Shelfbreak Front. Large inshore movements of the front give Black Sea Bass an energetic advantage by decreasing the distance needed to travel from their summer habitat (Miller et al. 2016a).

Golden tilefish are another species that may be affected by the movement of the Shelfbreak Front. Tilefish are benthic species that live predominantly along the shelfbreak within a narrow temperature band (Dawson 2021). They are thought to be susceptible to environmental variability, particularly during recruitment, with catch-per-unit-effort being linked to the Atlantic Multidecadal Oscillation, North Atlantic Oscillation, Gulf Stream position, and Labrador current flow at lagged timescales (Nesslage et al. 2021). This particular suite of environmental drivers can affect tilefish through changes in water properties along the shelfbreak, with relatively warmer waters being advantageous and

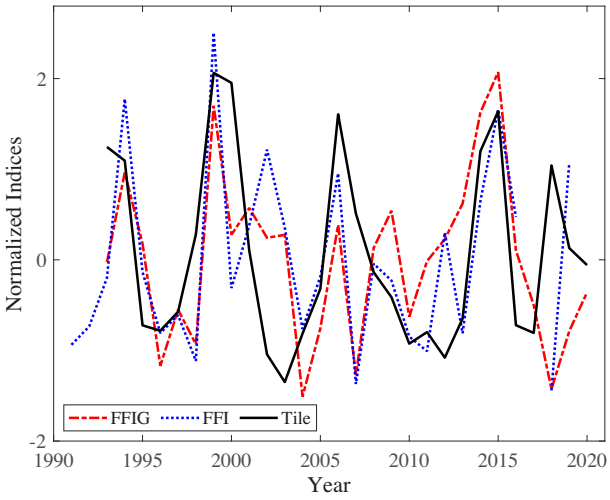

Figure 6. Golden tilefish recruitment estimate from an Age Structured Assessment Program model (Legault and Restrepo 1998) is shown in the solid black line compared to the fall values from the observational front index (FFI) and the GLORYS front index (FFIG) in blue dotted and red dashed lines, respectively.

colder waters being detrimental. For instance, there was a large-scale die-off observed in the spring of 1882 that was linked to a cold water event (Fisher et al. 2014). Therefore, movement of the Shelfbreak Front is thought to expand or contract suitable tilefish habitat, affecting recruitment. To investigate this relationship as a preliminary proof of concept, we compared our index estimates of the front position in fall (a season found to be important for tilefish recruitment) to the tilefish recruitment estimate developed as part of the 2021 Management Track Assessment for golden tilefish in the Mid-Atlantic/Southern New England region (Nitschke 2021, NEFSC 2022). The recruitment estimate is a model output generated from an Age Structured Assessment Program (ASAP) model (Legault and Restrepo 1998) and estimates the relative abundance of one-year-old tilefish. For more information on the recruitment estimate, we refer people to the final Management Track Assessment report, which is available on NOAA Fisheries Stock Status, Management, Assessment, and Resource Trends web tool (Stock SMART: https://apps-st.fisheries.noaa.gov/stocksmart?stockname=Tilefish%20-%20Mid-Atlantic%20Coast&stockid=10385). We found a correlation of $r = 0.40$ and 0.43 between the recruitment index and the FFI and FFIG, respectively. Though these correlation values are relatively low, the frontal indices effectively capture the high recruitment pulses that occur (Fig. 6). Given the 5–7-year lag between the time of recruitment and when tilefish enter the fishery, these frontal indices could provide valuable insights for understanding the population dynamics of this relatively data-poor species. If the relationship between the frontal indices and tilefish recruitments holds, then these indices could potentially be used to help improve population abundance forecasts, which are essential for sustainable fisheries management.

Oceanographic indices have been incorporated into general additive models to understand the relationship between oceanographic drivers and catch-per-unit-effort (Salois et al. 2023). Future studies utilizing similar physics-informed indices of oceanographic variability, such as those developed

here, may help better understand how the movement of the Shelfbreak Front could affect benthic species in the Middle Atlantic Bight.

Acknowledgments

We gratefully acknowledge the efforts of NOAA's Northeast Fisheries Science Center for running the Ecosystem Monitoring Program, which provided the majority of the CTD used within the study. We are grateful to Copernicus Marine Services for making the GLORYS reanalysis and sea surface height data publicly available.

Author contributions

A.S. wrote the manuscript with contributions from H.O., G.G., P.F., and S.S. in both manuscript editing and conceptualization. A.S., H.O., G.G., P.F., and S.S. helped with hypothesis generation, with A.S. completing the data curation and figure generation.

Supplementary data

Supplementary material is available at the *ICES Journal of Marine Science* online.

Conflict of interest: None declared.

Funding

A.S., G.G., and H.O. are grateful for financial support from NOAA (NA24OARX431C0019). A.S. was also supported by WHOI, and G.G. was supported by NSF (OCE-2122726).

Data availability

CTD profiles can be downloaded from the World Ocean Database (WOD) (Boyer et al. 2018, https://www.ncei.noaa.gov/products/world-ocean-database). Both the reanalysis product GLORYS12V1 reanalysis product (GLORYS; doi: https://doi.org/10.48670/moi-00021) and the gridded daily sea surface height data (doi: https://doi.org/10.48670/moi-00148) are available through Copernicus Marine Services.

References

[NEFSC] Northeast Fisheries Science Center. Management track assessment June 2021. *Northeast Fisheries Science Center Reference Document*. 2022;**22–10**:79.

Amante C, Eakins BW. ETOPO1 1 Arc-minute Global Relief model: procedures, Data sources and analysis. NOAA Technical Memorandum NESDIS NGDC-24. *National Geophysical Data Center, NOAA*. 2009. https://doi.org/10.7289/V5C8276M [March 23, 2023]

Beardsley RC, Chapman DC, Brink KH *et al.* The Nantucket Shoals flux experiment (NSFE79). Part I: a basic description of the current and temperature variability. *J Phys Oceanogr* 1985;**15**:713–48. https://doi.org/10.1175/1520-0485(1985)015%3c0713:TNSFEP%3e2.0.CO;2

Boyer TP, Baranova OK, Coleman C *et al.* 2018. World Ocean Database 2018. A.V. Mishonov, Technical Ed., NOAA Atlas NESDIS 87. https://www.ncei.noaa.gov/products/world-ocean-database [July 18, 2023]

Castillo-Trujillo AC, Kwon YO, Fratantoni P *et al.* An evaluation of eight global ocean reanalyses for the Northeast US continental shelf. *Prog Oceanogr* 2023;**219**:103126. https://doi.org/10.1016/j.pocean.2023.103126

Chapman DC, Lentz SJ. Trapping of a coastal density front by the bottom boundary layer. *Journal of Physical Oceanography* 1994;**24**:1464–1479. https://doi.org/10.1175/1520-0485(1994)024(1464:TOACDF)2.0.CO;2

Chen K, Gawarkiewicz G, Yang J. Mesoscale and submesoscale shelf-ocean exchanges initialize an advective marine heatwave. *J Geophys Res Oceans* 2022;**127**:e2021JC017927. https://doi.org/10.1029/2021JC017927

Chen Z, Kwon YO, Chen K *et al.* Seasonal prediction of bottom temperature on the northeast US continental shelf. *J Geophys Res Oceans* 2021;**126**:e2021JC017187. https://doi.org/10.1029/2021JC017187

Dawson KM. *Age, Growth, and Otolith Microchemistry of Golden Tilefish (Lopholatilus chamaeleonticeps) in the NW Atlantic*. Doctoral dissertation, Michigan Technological University, 2021. https://doi.org/10.37099/mtu.dc.etdr/1263

Fisher JA, Frank KT, Petrie B *et al.* Life on the edge: environmental determinants of tilefish (*Lopholatilus chamaeleonticeps*) abundance since its virtual extinction in 1882. *ICES J Mar Sci* 2014;**71**:2371–8. https://doi.org/10.1093/icesjms/fsu053

Flagg CN, Beardsley RC. On the stability of the shelf water/slope water front south of New England. *Journal of Geophysical Research: Oceans*. 1978;**83**(C9):4623–31. https://doi.org/10.1029/JC083iC09p04623

Flagg CN, Dunn M, Wang DP *et al.* A study of the currents of the outer shelf and upper slope from a decade of shipboard ADCP observations in the Middle Atlantic Bight. *J Geophys Res Oceans* 2006;**111**:C06003. https://doi.org/10.1029/2005JC003116

Forsyth J, Andres M, Gawarkiewicz G. Shelfbreak jet structure and variability off New Jersey using ship of opportunity data from the CMV oleander. *J Geophys Res Oceans* 2020;**125**:e2020JC016455. https://doi.org/10.1029/2020JC016455

Forsyth J, Gawarkiewicz G, Andres M. The impact of warm core rings on Middle Atlantic Bight shelf temperature and shelf break velocity. *J Geophys Res Oceans* 2022;**127**:e2021JC017759. https://doi.org/10.1029/2021JC017759

Forsyth JST, Andres M, Gawarkiewicz GG. Recent accelerated warming of the continental shelf off New Jersey: observations from the CMV Oleander expendable bathythermograph line. *J Geophys Res Oceans* 2015;**120**:2370–84. https://doi.org/10.1002/2014JC010516

Fratantoni PS, Pickart RS. The western North Atlantic shelfbreak current system in summer.*Journal of Physical Oceanography* 2007;**37**:2509–2533. https://doi.org/10.1175/JPO3123.1

Fratantoni PS, Pickart RS. Variability of the shelf break jet in the Middle Atlantic Bight: internally or externally forced? *J Geophys Res Oceans* 2003;**108**. 3166. https://doi.org/10.1029/2002JC001326

Gangopadhyay A, Gawarkiewicz G, Silva ENS *et al.* A census of the warm-core rings of the Gulf Stream: 1980–2017. *J Geophys Res Oceans* 2020;**125**:e2019JC016033. https://doi.org/10.1029/2019JC016033

Gangopadhyay A, Gawarkiewicz G, Silva ENS *et al.* An observed regime shift in the formation of warm core rings from the Gulf Stream. *Sci Rep* 2019;**9**:12319. https://doi.org/10.1038/s41598-019-48661-9

Gawarkiewicz G, Brink KH, Bahr F *et al.* A large-amplitude meander of the Shelfbreak Front during summer south of New England: observations from the Shelfbreak PRIMER experiment. *J Geophys Res Oceans* 2004;**109**. C03006. https://doi.org/10.1029/2002JC001468

Gawarkiewicz G, Chapman DC. The role of stratification in the formation and maintenance of shelf-break fronts. *J Phys Oceanogr* 1992;**22**:753–72. https://doi.org/10.1175/1520-0485(1992)022%3c0753:TROSIT%3e2.0.CO;2

Gawarkiewicz G, Chen K, Forsyth J *et al.* Characteristics of an advective marine heatwave in the Middle Atlantic Bight in early 2017.

Front Mar Sci 2019;**6**:712. https://doi.org/10.3389/fmars.2019.00712

Gawarkiewicz G, Fratantoni P, Bahr F *et al.* Increasing frequency of mid-depth salinity maximum intrusions in the Middle Atlantic bight. *J Geophys Res Oceans* 2022;**127**:e2021JC018233. https://doi.org/10.1029/2021JC018233

Gawarkiewicz G, Todd RE, Zhang W *et al.* The changing nature of shelf-break exchange revealed by the OOI Pioneer Array. *Oceanography* 2018;**31**:60–70. https://doi.org/10.5670/oceanog.2018.110

Harden BE, Gawarkiewicz GG, Infante M. Trends in physical properties at the southern New England shelf break. *J Geophys Res Oceans* 2020;**125**:e2019JC015784. https://doi.org/10.1029/2019JC015784

Hart DR. Effects of sea stars and crabs on sea scallop *Placopecten magellanicus* recruitment in the Mid-Atlantic Bight (USA). *Mar Ecol Prog Ser* 2006;**306**:209–21. https://doi.org/10.3354/meps306209

Houghton RW, Aikman F, Ou HW. Shelf-slope frontal structure and cross-shelf exchange at the New England shelf-break. *Cont Shelf Res* 1988;**8**:687–710. https://doi.org/10.1016/0278-4343(88)90072-6

Houghton RW, Flagg CN, Pietrafesa LJ. Shelf-slope water frontal structure, motion and eddy heat flux in the southern Middle Atlantic Bight. *Deep Sea Res Part II* 1994;**41**:273–306. https://doi.org/10.1016/0967-0645(94)90024-8

Houghton RW, Visbeck M. Upwelling and convergence in the Middle Atlantic Bight Shelfbreak front. *Geophys Res Lett* 1998;**25**:2765–8. https://doi.org/10.1029/98GL02105

Joyce TM, Bishop JK, Brown OB. Observations of offshore shelf-water transport induced by a warm-core ring. *Deep Sea Res A* 1992;**39**:S97–S113. https://doi.org/10.1016/S0198-0149(11)80007-5

Kavanaugh MT, Rheuban JE, Luis KM *et al.* Thirty-three years of ocean benthic warming along the US northeast continental shelf and slope: patterns, drivers, and ecological consequences. *J Geophys Res Oceans* 2017;**122**:9399–414. https://doi.org/10.1002/2017JC012953

Kleisner KM, Fogarty MJ, McGee S *et al.* Marine species distribution shifts on the US Northeast Continental Shelf under continued ocean warming. *Prog Oceanogr* 2017;**153**:24–36. https://doi.org/10.1016/j.pocean.2017.04.001

Legault CM, Restrepo VR. A flexible forward age-structured assessment program **49**, *Collect. Vol. Sci. Pap. ICCAT*. 1998, 246–53. https://sedarweb.org/documents/s12rd06-a-flexible-forward-age-structured-assessment-program/

National Marine Fisheries Service. Fisheries of the United States, 2020. U.S. Department of Commerce, NOAA Current Fishery Statistics No. 2022. 2024; https://www.fisheries.noaa.gov/national/sustainable-fisheries/fisheries-united-states

Linder CA, Gawarkiewicz G. A climatology of the Shelfbreak Front in the Middle Atlantic Bight. *J Geophys Res Oceans* 1998;**103**:18405–23. https://doi.org/10.1029/98JC01438

Manning J. Middle Atlantic Bight salinity: interannual variability. *Cont Shelf Res* 1991;**11**:123–37, https://doi.org/10.1016/0278-4343(91)90058-E

McHenry J, Welch H, Lester SE *et al.* Projecting marine species range shifts from only temperature can mask climate vulnerability. *Glob Chang Biol* 2019;**25**:4208–21. https://doi.org/10.1111/gcb.14828

Miller AS, Shepherd GR, Fratantoni PS. Offshore habitat preference of overwintering juvenile and adult black sea bass, *Centropristis striata*, and the relationship to year-class success. *PLoS One* 2016a;**11**:e0147627. https://doi.org/10.1371/journal.pone.0147627

Miller TJ, Hare JA, Alade LA. A state-space approach to incorporating environmental effects on recruitment in an age-structured assessment model with an application to southern New England yellowtail flounder. *Can J Fish Aquat Sci* 2016b;**73**:1261–70. https://doi.org/10.1139/cjfas-2015-0339

Mills KE, Pershing AJ, Brown CJ *et al.* Fisheries management in a changing climate: lessons from the 2012 ocean heat wave in the Northwest Atlantic. *Oceanography* 2013;**26**:191–5. https://doi.org/10.5670/oceanog.2013.27

Morley JW, Selden RL, Latour RJ *et al.* Projecting shifts in thermal habitat for 686 species on the North American continental shelf. *PLoS One* 2018;**13**:e0196127. https://doi.org/10.1371/journal.pone.0196127

Mountain DG. Variability in the properties of Shelf Water in the Middle Atlantic Bight, 1977–1999. *J Geophys Res Oceans* 2003;**108**: 14–1. https://doi.org/10.1029/2001JC001044

Nesslage G, Lyubchich V, Nitschke P *et al.* Environmental drivers of golden tilefish (*Lopholatilus chamaeleonticeps*) commercial landings and catch-per-unit-effort. *Fish Oceanogr* 2021;**30**:608–22. https://doi.org/10.1111/fog.12540

Neto AG, Langan JA, Palter JB. Changes in the Gulf Stream preceded rapid warming of the Northwest Atlantic Shelf. *Commun Earth Environ* 2021;**2**:74. https://doi.org/10.1038/s43247-021-00143-5

Nitschke P. Golden Tilefish, Lopholatilus chamaeleonticeps, Management Track Assessment through 2020 in the Middle Atlantic-Southern New England Region. *Northeast Fisheries Science Center* 2021. https://repository.library.noaa.gov/view/noaa/39406

Pershing AJ, Alexander MA, Hernandez CM *et al.* Slow adaptation in the face of rapid warming leads to collapse of the Gulf of Maine cod fishery. *Science* 2015;**350**:809–12. https://doi.org/10.1126/science.aac9819

Pickart RS, Torres DJ, McKee TK *et al.* Diagnosing a meander of the shelf break current in the Middle Atlantic Bight. *J Geophys Res Oceans* 1999;**104**:3121–32. https://doi.org/10.1029/1998JC900066

Salois SL, Hyde KJ, Silver A *et al.* Shelf break exchange processes influence the availability of the northern shortfin squid, *Illex illecebrosus*, in the Northwest Atlantic. *Fish Oceanogr* 2023;**32**:461–78. https://doi.org/10.1111/fog.12640

Silver A, Gangopadhyay A, Gawarkiewicz G *et al.* Increased gulf stream warm core ring formations contributes to an observed increase in salinity maximum intrusions on the Northeast Shelf. *Sci Rep* 2023;**13**:7538. https://doi.org/10.1038/s41598-023-34494-0

Silver A, Gangopadhyay A, Gawarkiewicz G *et al.* Interannual and seasonal asymmetries in Gulf Stream ring formations from 1980 to 2019. *Sci Rep* 2021;**11**:2207. https://doi.org/10.1038/s41598-021-81827-y

Silver A, Gangopadhyay A, Gawarkiewicz G *et al.* Spatial variability of movement, structure, and formation of warm core rings in the northwest Atlantic Slope sea. *J Geophys Res Oceans* 2022;**127**:e2022JC018737. https://doi.org/10.1029/2022JC018737

Smith KE, Burrows MT, Hobday AJ *et al.* Socioeconomic impacts of marine heatwaves: global issues and opportunities. *Science* 2021;**374**:eabj3593. https://doi.org/10.1126/science.abj3593

Stewart PL, Arnold SH. Environmental requirements of the sea scallop (*Placopecten magellanicus*) in eastern Canada and its response to human impacts. *Can Tech Rep Fish Aquat Sci* 1994;**2005**:1–36. https://publications.gc.ca/site/eng/9.579045/publication.html

Tanaka KR, Torre MP, Saba VS *et al.* An ensemble high-resolution projection of changes in the future habitat of American lobster and sea scallop in the Northeast US continental shelf. *Divers Distrib* 2020;**26**:987–1001. https://doi.org/10.1111/ddi.13069

Ullman DS, Cornillon PC. Satellite-derived sea surface temperature fronts on the continental shelf off the northeast US coast. *J Geophys Res Oceans* 1999;**104**:23459–78. https://doi.org/10.1029/1999JC900133

Wright DG. On the alongshelf evolution of an idealized density front. *J Phys Oceanogr* 1989;**19**:532–41. https://doi.org/10.1175/1520-0485(1989)019%3c0532:OTAEOA%3e2.0.CO;2

Wright WR. The limits of shelf water south of Cape Cod, 1941 to 1972. *J Mar Res* 1976;**34**:1–14. https://elischolar.library.yale.edu/journal_of_marine_research/1343

Yankovsky AE, Chapman DC. A simple theory for the fate of buoyant coastal discharges. *J Phys Oceanogr* 1997;**27**:1386–401. https://doi.org/10.1175/1520-0485(1997)027%3c1386:ASTFTF%3e2.0.CO;2

Zhang WG, Alatalo P, Crockford T *et al.* Cross-shelf exchange associated with a shelf-water streamer at the Mid-Atlantic Bight shelf edge. *Prog Oceanogr* 2023;**210**:102931. https://doi.org/10.1016/j.pocean.2022.102931

Zhang WG, McGillicuddy DJ, Gawarkiewicz GG. Is biological productivity enhanced at the New England Shelfbreak Front? *J Geophys Res Oceans* 2013;**118**:517–35. https://doi.org/10.1002/jgrc.20068

Handling Editor: Matthew Oliver